Chirality and octupole correlations in ^{74}As

X. Xiao (肖骁),[1] S. Y. Wang (王守宇) ⓞ,[1,*] C. Liu (刘晨),[1,†] R. A. Bark,[2] J. Meng (孟杰),[3,4,5] S. Q. Zhang (张双全),[3]
B. Qi (亓斌),[1] H. Hua (华辉),[3] P. Jones,[2] S. M. Wyngaardt,[5] S. Wang (王硕),[1] D. P. Sun (孙大鹏),[1] Z. Q. Li (李志泉),[1]
N. B. Zhang (张乃波),[1] H. Jia (贾慧),[1] R. J. Guo (郭睿巨),[1] X. C. Han (韩星池),[1] L. Mu (穆琳),[1] X. Lu (陆晓),[1]
W. Z. Xu (许文政),[1] C. Y. Niu (牛晨阳),[3] C. G. Wang (王春光),[3] E. A. Lawrie,[2,6] J. J. Lawrie,[2,6] J. F. Sharpey-Schafer,[2,6]
M. Wiedeking,[2,7] S. N. T. Majola,[2,8] T. D. Bucher,[2,5] T. Dinoko,[9] B. Maqabuka,[2,6] L. Makhathini,[2,5] L. Mdletshe,[2,10]
N. A. Khumalo,[2,6] O. Shirinda,[2,11] and K. Sowazi[2]

[1]*Shandong Provincial Key Laboratory of Optical Astronomy and Solar-Terrestrial Environment, Institute of Space Sciences,*
Shandong University, Weihai 264209, People's Republic of China
[2]*iThemba LABS, Somerset West 7129, South Africa*
[3]*School of Physics and State Key Laboratory of Nuclear Physics and Technology,*
Peking University, Beijing 100871, People's Republic of China
[4]*School of Physics and Nuclear Energy Engineering, Beihang University, Beijing 100191, People's Republic of China*
[5]*Department of Physics, University of Stellenbosch, Matieland 7602, South Africa*
[6]*Physics Department, University of the Western Cape, Private Bag X17, Bellville 7535, South Africa*
[7]*School of Physics, University of the Witwatersrand, Johannesburg 2050, South Africa*
[8]*Department of Physics, University of Cape Town, Rondebosch 7700, South Africa*
[9]*Department of Physical and Electrical Metrology, NMISA, Private Bag X34, Lynnwood Ridge, Pretoria, 0040, South Africa*
[10]*University of Zululand, Private Bag X1001, KwaDlangezwa 3886, South Africa*
[11]*Department of Physical and Earth Sciences, Sol Plaatje University, Private Bag X5008, Kimberley 8301, South Africa*

High-spin states in ^{74}As were studied using the ^{74}Ge(^{4}He, $1p3n$) reaction at beam energies of 58.6 and 62.6
MeV. Two positive- and one negative-parity bands have been identified in ^{74}As. The two positive-parity bands are
interpreted as chiral doublet bands, which is supported by the triaxial particle rotor model. Three electric dipole
transitions linking the yrast positive- and negative-parity bands were also observed in this work, suggesting the
existence of octupole correlations in ^{74}As.

I. INTRODUCTION

Chirality in nuclei was first proposed by Frauendorf and
Meng in 1997 [1]. They pointed out that the rotation of tri-
axial nuclei may demonstrate chiral symmetry, and result in
pairs of nearly degenerate $\Delta I = 1$ bands with the same parity,
i.e., chiral doublet bands [1]. From then on, theoretical and
experimental studies were carried out widely on the subject of
nuclear chirality. In 2006, covariant density functional theory
(CDFT) calculations suggested that multiple chiral doublet
(MχD) bands can exist in a single nucleus [2]. So far, experi-
mental evidence for candidate chiral doublet bands, including
MχD bands, has been found in the $A \approx 80$, 100, 130, and 190
mass regions, as discussed in Refs. [3–9].

The $A \approx 80$ mass region is a recently identified chiral re-
gion where five nuclei with candidate chiral bands have been
reported [10–14]. Chiral doublet bands were first reported in
the Br isotopes [10–12] in this mass region. Subsequently,
chiral doublet bands were reported in ^{84}Rb [13] and ^{81}Kr [14].
The observation of these chiral nuclei makes the $A \approx 80$ mass

region a new chiral island. It is naturally interesting to explore
the boundaries of the chirality in the $A \approx 80$ mass region.

Recently, MχD bands with octupole correlations were
found in ^{78}Br [11], which indicated that chiral and reflec-
tion symmetry can be simultaneously breaking and nuclear
chirality can be robust against the octupole correlations. The
experimental observation has motivated corresponding theo-
retical studies [15,16] on the simultaneous breaking of chiral
and reflection symmetries in nuclei. Up to now, the coexis-
tence of chirality and octupole correlations in a nucleus has
been reported in ^{78}Br [11], ^{124}Cs [17], and ^{131}Ba [18].

In order to explore the boundaries of the chiral nuclei in
the $A \approx 80$ mass region and investigate the coexistence of
chirality and octupole correlations, we carried out a series
of experimental studies in the 80 mass region as mentioned
above. In this paper, we report on a coexistence of chiral-
ity and octupole correlations in ^{74}As, and extend the low Z
boundaries of the chiral nuclei in the $A \approx 80$ mass region to
the $Z = 33$ As isotopes for the first time.

II. EXPERIMENTAL DETAILS

High-spin states of ^{74}As were populated via the reaction
^{74}Ge(^{4}He, $1p3n$) at beam energies of 58.6 and 62.6 MeV.

*sywang@sdu.edu.cn
†cliu@sdu.edu.cn

TABLE I. γ-ray energies, spin-parity assignments and excitation energies for the initial and final states, relative intensities, ADO ratios, and A_p values of the transitions in ^{74}As. The γ-ray energies are accurate to ± 0.5 keV.

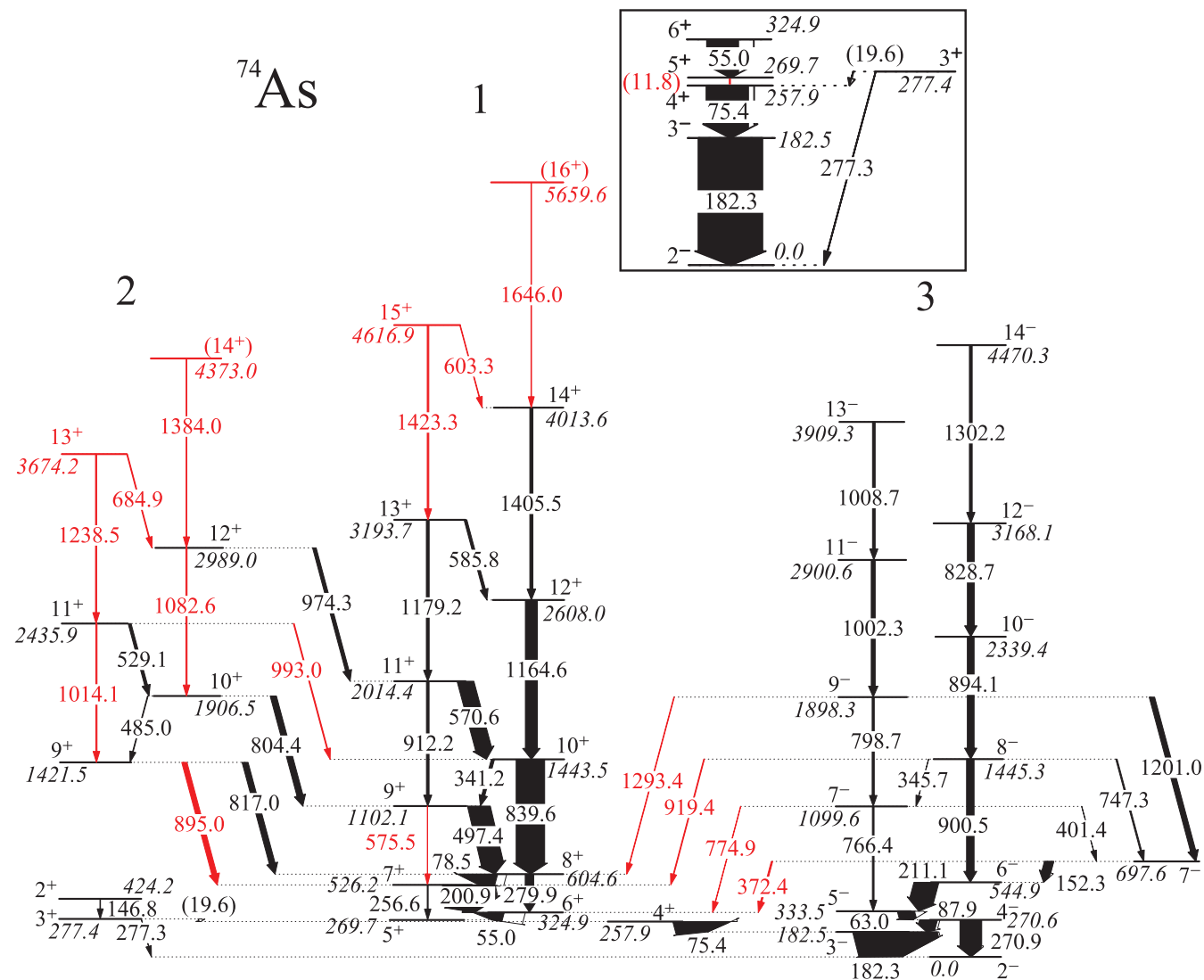| E_γ (keV)	$I_i^\pi \rightarrow I_f^\pi$	E_i (keV) $\rightarrow E_f$ (keV)	I_γ	R_{ADO}	A_p
(19.6)	$3^+ \rightarrow 4^+$	$277.4 \rightarrow 257.9$	<0.2[a]		
55.0	$6^+ \rightarrow 5^+$	$324.9 \rightarrow 269.7$	49.7(20.2)[a]		
63.0	$5^- \rightarrow 4^-$	$333.5 \rightarrow 270.6$	20.3(10.0)[a]		
75.4	$4^+ \rightarrow 3^-$	$257.9 \rightarrow 182.5$	66.4(12.4)[a]		
78.5	$8^+ \rightarrow 7^+$	$604.6 \rightarrow 526.2$	48.7(11.8)[a]		
87.9	$4^- \rightarrow 3^-$	$270.6 \rightarrow 182.5$	21.1(16.9)[a]		
146.8	$2^+ \rightarrow 3^+$	$424.2 \rightarrow 277.4$	0.6(0.2)		
152.3	$7^- \rightarrow 6^-$	$697.6 \rightarrow 544.9$	10.7(2.7)	0.85(0.16)	$-0.08(0.04)$
182.3	$3^- \rightarrow 2^-$	$182.5 \rightarrow 0.0$	100.0(11.5)	0.81(0.13)	$-0.07(0.02)$
200.9	$7^+ \rightarrow 6^+$	$526.2 \rightarrow 324.9$	62.1(12.1)	0.73(0.11)	$-0.08(0.01)$
211.1	$6^- \rightarrow 5^-$	$544.9 \rightarrow 333.5$	29.4(5.6)	0.86(0.12)	$-0.11(0.01)$
256.6	$7^+ \rightarrow 5^+$	$526.2 \rightarrow 269.7$	1.1(0.3)	1.19(0.14)	
270.9	$4^- \rightarrow 2^-$	$270.6 \rightarrow 0.0$	26.0(6.0)	1.23(0.13)	0.09(0.01)
277.3	$3^+ \rightarrow 2^-$	$277.4 \rightarrow 0.0$	0.2(0.1)		
279.9	$8^+ \rightarrow 6^+$	$604.6 \rightarrow 324.9$	10.2(2.4)	1.14(0.12)	0.11(0.06)
341.2	$10^+ \rightarrow 9^+$	$1443.5 \rightarrow 1102.1$	3.7(0.7)	0.69(0.06)	$-0.03(0.04)$
345.7	$8^- \rightarrow 7^-$	$1445.3 \rightarrow 1099.6$	0.3(0.2)		
372.4	$7^- \rightarrow 6^+$	$697.6 \rightarrow 324.9$	1.7(0.4)	0.75(0.06)	0.06(0.05)
401.4	$7^- \rightarrow 7^-$	$1099.6 \rightarrow 697.6$	0.3(0.1)		
485.0	$10^+ \rightarrow 9^+$	$1906.5 \rightarrow 1421.5$	0.8(0.3)		
497.4	$9^+ \rightarrow 8^+$	$1102.1 \rightarrow 604.6$	27.1(4.5)	0.71(0.03)	$-0.05(0.01)$
529.1	$11^+ \rightarrow 10^+$	$2435.9 \rightarrow 1906.5$	2.0(0.8)	0.63(0.03)	$-0.12(0.05)$
570.6	$11^+ \rightarrow 10^+$	$2014.4 \rightarrow 1443.5$	19.8(5.2)	0.73(0.03)	$-0.04(0.01)$
575.5	$9^+ \rightarrow 7^+$	$1102.1 \rightarrow 526.2$	<0.2		
585.8	$13^+ \rightarrow 12^+$	$3193.7 \rightarrow 2608.0$	3.3(1.8)	0.74(0.06)	$-0.08(0.03)$
603.3	$15^+ \rightarrow 14^+$	$4616.9 \rightarrow 4013.6$	0.7(0.4)		
684.9	$13^+ \rightarrow 12^+$	$3674.2 \rightarrow 2989.0$	1.0(0.6)		
747.3	$8^- \rightarrow 7^-$	$1445.3 \rightarrow 697.6$	1.6(0.6)	0.63(0.14)	
766.4	$7^- \rightarrow 5^-$	$1099.6 \rightarrow 333.5$	2.0(0.4)	1.10(0.06)	0.06(0.03)
774.9	$7^- \rightarrow 6^+$	$1099.6 \rightarrow 324.9$	0.5(0.1)		
798.7	$9^- \rightarrow 7^-$	$1898.3 \rightarrow 1099.6$	2.6(1.0)	1.29(0.17)	0.14(0.06)
804.4	$10^+ \rightarrow 9^+$	$1906.5 \rightarrow 1102.1$	7.4(1.4)	0.63(0.02)	$-0.02(0.02)$
817.0	$9^+ \rightarrow 8^+$	$1421.5 \rightarrow 604.6$	7.1(1.2)	0.60(0.02)	$-0.02(0.02)$
828.7	$12^- \rightarrow 10^-$	$3168.1 \rightarrow 2339.4$	8.3(2.4)	1.24(0.04)	0.19(0.05)
839.6	$10^+ \rightarrow 8^+$	$1443.5 \rightarrow 604.6$	34.7(5.7)	1.17(0.05)	0.06(0.01)
894.1	$10^- \rightarrow 8^-$	$2339.4 \rightarrow 1445.3$	8.2(2.4)	1.30(0.03)	0.08(0.02)
895.0	$9^+ \rightarrow 7^+$	$1421.5 \rightarrow 526.2$	6.1(1.0)	1.16(0.03)	0.06(0.04)
900.5	$8^- \rightarrow 6^-$	$1445.3 \rightarrow 544.9$	9.1(2.6)	1.28(0.02)	0.10(0.01)
912.2	$11^+ \rightarrow 9^+$	$2014.4 \rightarrow 1102.1$	3.2(0.6)	1.21(0.08)	0.11(0.04)
919.4	$8^- \rightarrow 7^+$	$1445.3 \rightarrow 526.2$	0.9(0.3)		
974.3	$12^+ \rightarrow 11^+$	$2989.0 \rightarrow 2014.4$	4.2(2.0)	0.83(0.06)	$-0.49(0.19)$
993.0	$11^+ \rightarrow 10^+$	$2435.9 \rightarrow 1443.5$	1.0(0.3)		
1002.3	$11^- \rightarrow 9^-$	$2900.6 \rightarrow 1898.3$	4.8(1.9)	1.35(0.07)	0.16(0.05)
1008.7	$13^- \rightarrow 11^-$	$3909.3 \rightarrow 2900.6$	3.2(1.3)	1.19(0.15)	0.11(0.04)
1014.1	$11^+ \rightarrow 9^+$	$2435.9 \rightarrow 1421.5$	1.4(0.9)	1.23(0.04)	
1082.6	$12^+ \rightarrow 10^+$	$2989.0 \rightarrow 1906.5$	1.4(0.7)	1.36(0.33)	
1164.6	$12^+ \rightarrow 10^+$	$2608.0 \rightarrow 1443.5$	14.6(3.9)	1.24(0.07)	0.12(0.02)
1179.2	$13^+ \rightarrow 11^+$	$3193.7 \rightarrow 2014.4$	3.4(1.7)	1.27(0.07)	0.14(0.04)
1201.0	$9^- \rightarrow 7^-$	$1898.3 \rightarrow 697.6$	6.4(2.5)	1.22(0.03)	0.08(0.03)
1238.5	$13^+ \rightarrow 11^+$	$3674.2 \rightarrow 2435.9$	1.4(0.7)	1.32(0.3)	
1293.4	$9^- \rightarrow 8^+$	$1898.3 \rightarrow 604.6$	0.7(0.2)		
1302.2	$14^- \rightarrow 12^-$	$4470.3 \rightarrow 3168.1$	3.4(1.1)	1.11(0.10)	0.07(0.05)
1384.0	$(14^+) \rightarrow 12^+$	$4373.0 \rightarrow 2989.0$	0.8(0.4)		

TABLE I. (*Continued.*)

E_γ (keV)	$I_i^\pi \to I_f^\pi$	E_i (keV) $\to E_f$ (keV)	I_γ	R_{ADO}	A_p
1405.5	$14^+ \to 12^+$	$4013.6 \to 2608.0$	3.7(2.1)	1.08(0.07)	0.07(0.05)
1423.3	$15^+ \to 13^+$	$4616.9 \to 3193.7$	1.9(1.1)	1.34(0.09)	0.08(0.03)
1646.0	$(16^+) \to 14^+$	$5659.6 \to 4013.6$	0.7(0.4)		

aIntensities of the transitions are deduced from intensity balances. The internal conversion coefficients of the 55.0, 63.0, and 78.5 keV transitions, which are calculated using their mixing ratios based on the angular distribution measurements [30], are 0.500(0.324), 0.549(0.404), and 0.220(0.183), respectively. The internal conversion coefficients of the 75.4 and 87.9 keV transition are 0.144(0.020) and 0.137(0.015) [31], respectively.

The beam was delivered by the Separated Sector Cyclotron of iThemba LABS, South Africa. A 2.85 mg/cm^2 thick ^{74}Ge target with a 10.8 mg/cm^2 carbon backing was used in the experiment. The deexciting γ rays were detected by the AFRODITE array [19] which consisted of eight Compton suppressed clover detectors and two low-energy photon spectrometer (LEPS) detectors. Four clover detectors were positioned at 135° with respect to the beam axis, the other four and the two LEPS detectors were positioned at 90°. The energy and efficiency calibrations of the detectors were made using a standard ^{152}Eu radioactive source. Approximately 1.9×10^9 γ-γ coincidence events were accumulated

FIG. 1. Partial level scheme of ^{74}As established in the present work. The energies of the γ transitions and levels are given in keV. The measured relative intensities of transitions are proportional to the widths of the arrows. New transitions and levels are marked as red.
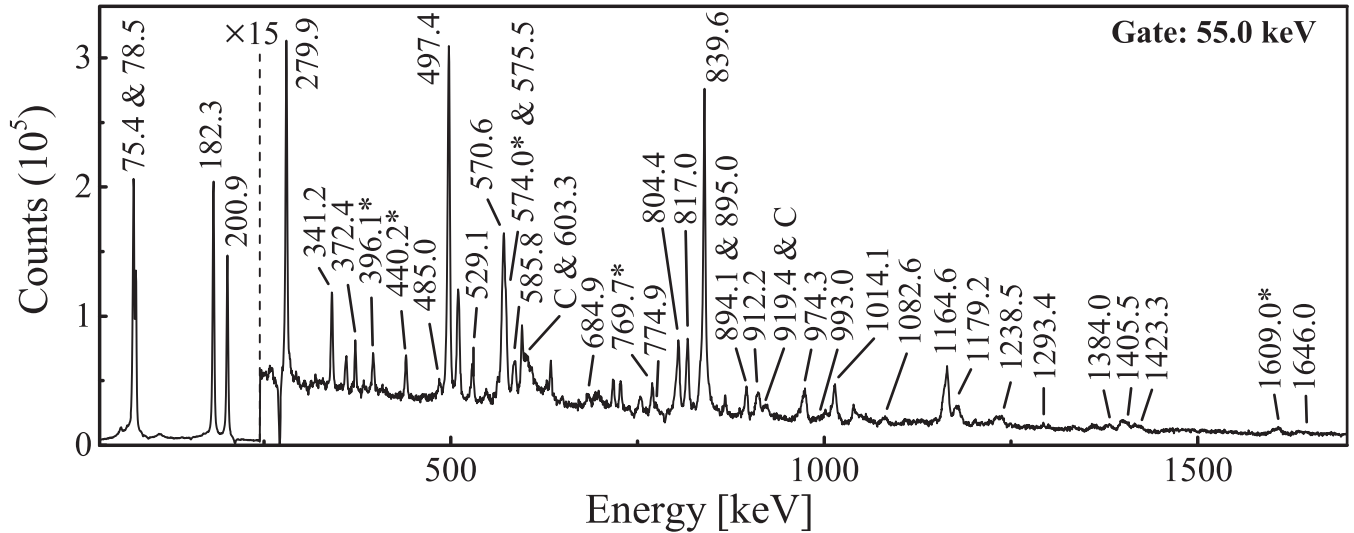
FIG. 2. A spectrum of γ rays gated on the 55.0 keV transition. The peaks marked with asterisks are transitions of ^{74}As but not included in Fig. 1, whereas those labeled with C are contaminations.

and sorted into a symmetric and several asymmetric matrices. The symmetric matrix was used for γ-γ coincidence analyses, and the asymmetric matrices were used to perform the angular distributions from the oriented states (ADO) [20] and the polarization asymmetry (A_p) measurements [21]. In the present geometry, typical ADO ratios ≈ 1.2 are expected for the stretched quadrupole or $\Delta I = 0$ dipole transitions and ≈ 0.8 for the stretched pure dipole transitions. The positive and negative A_p values correspond to the stretched electric or $\Delta I = 0$ magnetic transitions and the stretched magnetic transitions, respectively [21–23]. The obtained γ ray energies, spin-parity assignments for the initial and final states, relative intensities, ADO ratios, and A_p values of the transitions in ^{74}As are listed in Table I. More details of the experimental setup and procedure can be found in Ref. [24].

III. EXPERIMENTAL RESULTS

Prior to this work, the low-lying states of ^{74}As were studied in Refs. [25–31]. The 2^- ground state was assigned the $\pi f_{5/2} \otimes \nu g_{9/2}$ configuration [27]. An isomeric state with a lifetime of 26.8 ns was identified [28] and assigned the spin-parity of $I^\pi = 4^+$ [29]. Furthermore, high-spin states of ^{74}As were first reported in Ref. [32], in which a positive- and a negative-parity bands were established.

A partial level scheme of ^{74}As, derived from the present work, is presented in Fig. 1. As shown in Fig. 1, three $\Delta I = 1$ bands (labeled as 1–3) and a number of linking transitions are observed. In the present work, band 1 is extended to higher spins. Band 2 is established for the first time by adding five new transitions into the positive-parity sequence observed in Ref. [32], and it feeds into band 1 via five interband transitions. In addition, four new transitions of 372.4, 774.9, 919.4, and 1293.4 keV are observed linking the positive- and negative-parity level structures. Figure 2 shows the spectrum gated on the 55.0 keV transition. All the newly observed transitions can be seen in this figure. It should be noted that the newly observed 895.0 keV transition linking bands 1 and

2 is very close to the 894.1 keV transition in band 3. The two transitions can be distinguished by the specific γ-γ coincidence analysis. For example, we have gated on the 900.5, 55.0, and 1014.1 keV transitions and show the gated spectra in Fig. 3. The 894.1 and 895.0 keV transitions can be seen in
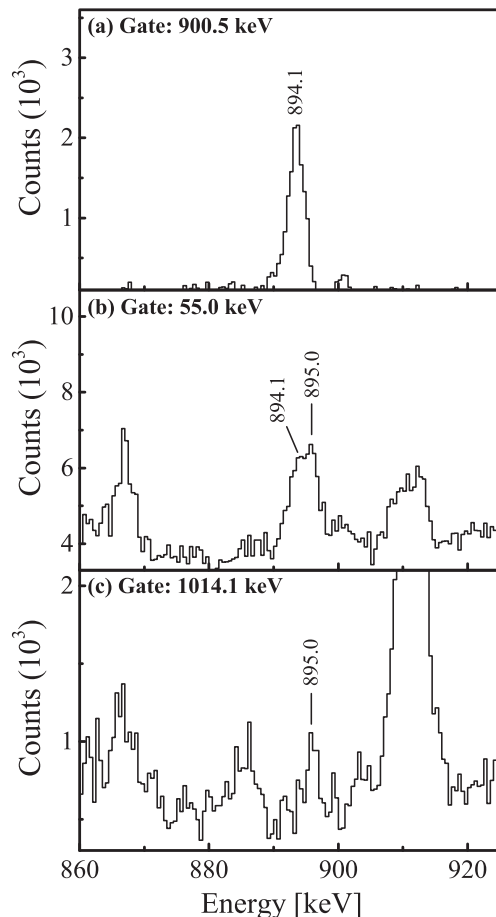

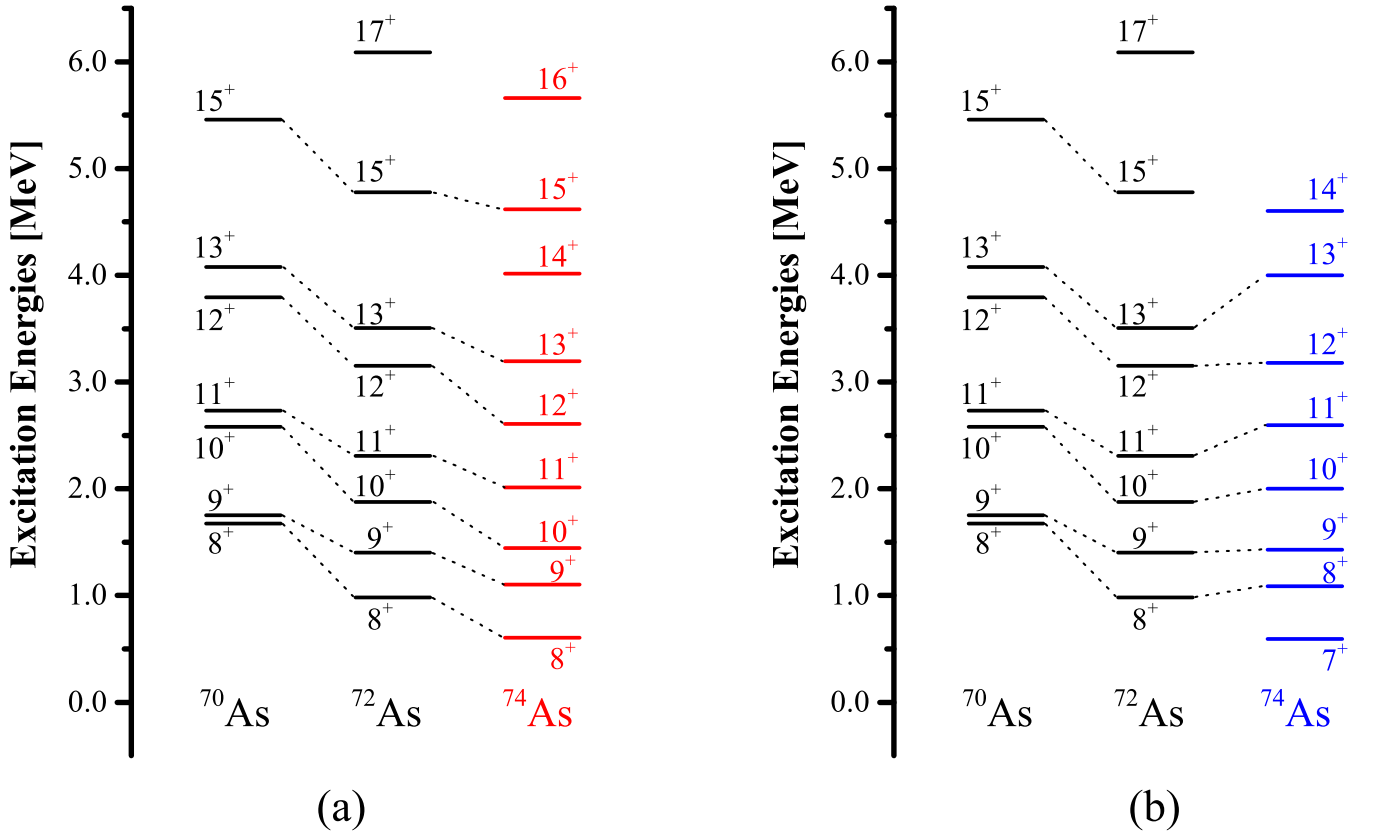FIG. 3. Spectra gated on 900.5, 55.0, and 1014.1 keV transitions.

FIG. 4. The systematics of the excitation energies for the yrast states above $I = 7$ in ^{70,72}As [33,34] and ^{74}As. The states of ^{74}As deduced from present work are marked as red, whereas those reported in Ref. [32] are marked as blue.

Figs. 3(a) and 3(c), respectively. In Fig. 3(b), both the 894.1 and 895.0 keV transitions can be seen. Therefore, the 895.0 keV transition is a different transition from the 894.1 keV transition.

The newly observed transitions of 1293.4, 919.4, 774.9 and 372.4 keV give rise to several new decay paths between the positive- and negative-parity level structures. Based on the energy conservation, a missing ≈11.8 keV energy gap exists somewhere between the level fed by the 372.4 keV transition and the ground state. The placements of the 19.6, 75.4, 182.3, 277.3 keV transitions have been fixed in Ref. [29], and the placement of the 55.0 keV transition has been fixed because of the existence of the 256.6 keV crossover transition. Thus, the energy gap can only exist between the 4^+ isomeric state and the final state of the 55.0 keV transition.

The spins and parities of the previously known low-lying states in ^{74}As were assigned based on the measurements of the β decay, angular distributions, and internal conversion coefficients of the γ rays [26,29,30], while those of the high-spin states were determined from the directional correlation of oriented states (DCO) ratios of the γ rays [32]. The present work has confirmed most of the multipolarity assignments of the known transitions, and assigned the multipolarities of the newly observed transitions by measuring ADO ratios and A_p values of the transitions. For example, the present work identified a 372.4 keV transition linking the first 7^- state and band 1. The measured ADO ratio and A_p value of the 372.4 keV linking transition are 0.75(0.06) and 0.06(0.05), respectively.

These values indicate that the 372.4 keV transition has an $E1$ character. We therefore assigned the spin-parity 6^+ to the final state of 372.4 keV transition. We have assigned the spins and parities of the other levels in ^{74}As based on the same method.

In the present work, the spins of the states in band 1 are $1\hbar$ larger than those in Ref. [32]. To examine the present spin assignments for the positive-parity level structures in ^{74}As, we performed a systematic comparison of the excitation energies of the yrast states above $I = 7$ in ^{70,72}As [33,34] with those in ^{74}As, and we present the results in Fig. 4. As shown in Fig. 4(a), based on the present spin-parity assignments, the excitation energies of levels with the same spins in ^{70,72,74}As show a smooth decrease as the neutron number increases. However, the excitation energies presented in Fig. 4(b) do not exhibit systematic trends. Thus, the systematic analysis supports the present spin assignments for the levels in ^{74}As.

IV. DISCUSSION

Band 1 had been assigned to the $\pi g_{9/2} \otimes \nu g_{9/2}$ configuration [32]. The newly established band 2 feeds into band 1 by four $M1/E2$ and an $E2$ linking transitions. The linking transitions should be strongly hindered unless the sidebands are built on the same configuration as main bands, as discussed in [35–37]. Thus, the observation of the $\Delta I = 1$ $M1/E2$ and $\Delta I = 2$ $E2$ linking transitions between bands 1 and 2 indicates that band 2 has the same $\pi g_{9/2} \otimes \nu g_{9/2}$ configuration as band 1.
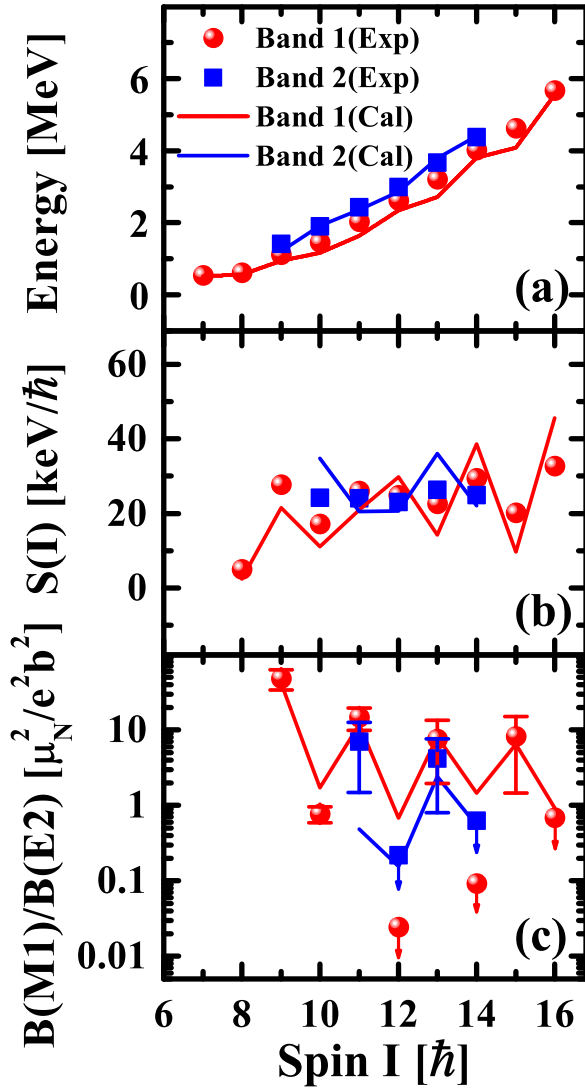
FIG. 5. The experimental excitation energies, energy stagger-ing parameters $S(I) = [E(I) - E(I-1)]/2I$, and reduced transition probability ratios $B(M1)/B(E2)$ for bands 1 and 2 in ^{74}As as func-tions of spin in comparison with the TPRM calculations.

To investigate the nature of bands 1 and 2, the exci-tation energies $E(I)$, energy staggering parameters $S(I) = [E(I) - E(I-1)]/2I$, and reduced transition probability ra-tios $B(M1)/B(E2)$ were extracted and presented in Fig. 5 as functions of spin. As shown in Fig. 5, bands 1 and 2 maintain an energy difference of ≈ 400 keV over the ob-served spin range. The two bands have similar $S(I)$ values, and the $S(I)$ exhibits a smooth variation versus spin. The $B(M1)/B(E2)$ values of bands 1 and 2 are close and show odd-even staggering. These experimental properties are sim-ilar to the positive-parity chiral doublet bands in ^{78,80,82}Br [10–12], and fulfill the fingerprints of the chiral doublet bands [3,38–40]. Therefore, we suggest that bands 1 and 2 are a pair of chiral doublet bands with the $\pi g_{9/2} \otimes \nu g_{9/2}$ configuration.

In order to further understand the chirality in ^{74}As, calcula-tions based on the triaxial particle rotor model (TPRM) [1,41–45] were performed. The TPRM is a quantum mechanical method that describes the system in the laboratory framework
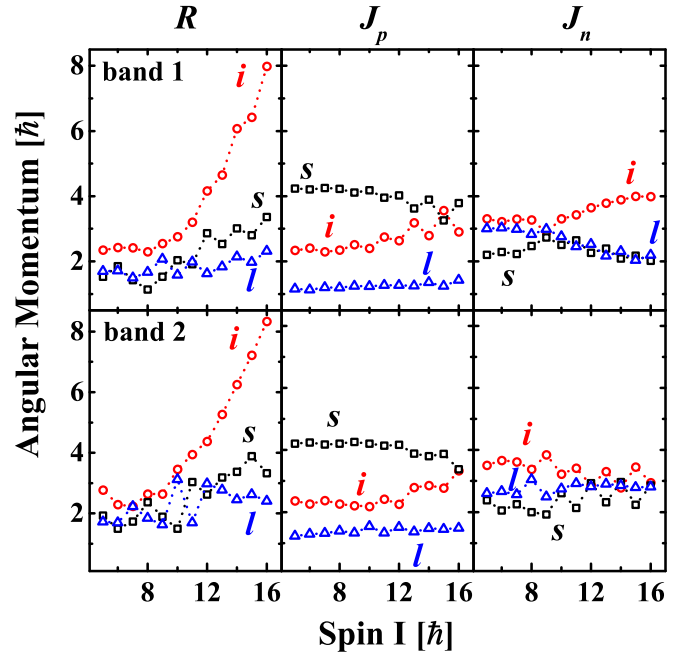

FIG. 6. The root-mean-square components along the intermedi-ate (i, circles), short (s, squares), and long (l, triangles) axes of the core, valence proton, and valence neutron angular momenta calcu-lated as functions of spin I by means of the TPRM for bands 1 and 2 in ^{74}As.

and yields directly the energy splitting and tunneling between doublet bands. It has been extensively used in the investigation of chiral doublet bands [46–48]. We obtained the deforma-tion parameters $(\beta_2, \gamma) = (0.37, 23.6°)$ for the $\pi g_{9/2} \otimes \nu g_{9/2}$ configuration from the previous relativistic mean-field (RMF) calculations [2,49]. The deformation parameter $\beta_2 = 0.37$ was used as input to the TPRM calculations. The triaxial deformation parameter γ and the moment of inertia $\mathcal{J}$ were adjusted to reproduce the experimental energy spectra and $B(M1)/B(E2)$ values, which occurred when $\gamma = 21.6°$ and $\mathcal{J} = 12 \ \hbar^2/$MeV. To preserve the number of particles, the proton Fermi surface was placed on the $\pi g_{9/2}[440]\frac{1}{2}$ or-bital, and the neutron Fermi surface was placed between the $\nu g_{9/2}[422]\frac{5}{2}$ and $\nu g_{9/2}[413]\frac{7}{2}$ orbitals. Other parameters in the TPRM were fixed following those in Refs. [41–44].

The calculated $E(I)$, $S(I)$, and $B(M1)/B(E2)$ ratios as functions of spin are presented in Fig. 5 and compared with the corresponding experimental data. As illustrated in Fig. 5, the small energy differences between bands 1 and 2 are well reproduced, and the calculated $S(I)$ are in good agreement with the available data, as well as the magnitude and the staggering phase of the $B(M1)/B(E2)$ ratios. The agreement between the experimental data and the calculations supports the present configuration assignment and allows us to further investigate the chiral geometry of the doublet bands in ^{74}As.

To study the chiral geometry of bands 1 and 2 in ^{74}As, similarly to the calculations in Refs. [10,12], the root-mean-quare values of the squared angular momenta components for the core R_k, the valence proton J_{pk}, and the valence neutron J_{nk} were calculated. The calculated results are presented in Fig. 6, in which $k = i, l, s$ represent the intermediate, long,

and short axes, respectively. As shown in Fig. 6, the angular momenta of the core and valence proton respectively align along the intermediate axis and the short axis, whereas the angular momentum of the valence neutron exhibits a large mixture between the three axes. For the ideal case of chiral geometry, the core, the valence proton, and the valence neutron mainly align their angular momenta along the intermediate, short, and long axes respectively [1,42,47,50,51]. Therefore, the coupling pattern of angular momenta in ^{74}As somewhat departs from the ideal chiral geometry, being attributed to the Fermi surface of the neutron placed between the $\nu g_{9/2}[422]\frac{5}{2}$ and $\nu g_{9/2}[413]\frac{7}{2}$ orbitals, instead of at the top of the $\nu g_{9/2}$ subshell. However, the total angular momentum is still aplanar, which supports the chiral interpretation for bands 1 and 2.

Three new $E1$ transitions linking bands 1 and 3 have been observed, implying the existence of octupole correlations in ^{74}As. To investigate the possible octupole correlations in ^{74}As, the experimental $B(E1)/B(E2)$ values and energy displacement δE [52,53] between bands 1 and 3 have been extracted and compared with those in ^{78}Br [11] and ^{224}Th [54] in Fig. 7. The positive- and negative-parity bands connected by $E1$ transitions in ^{78}Br were interpreted as evidence of octupole correlations [11], whereas the alternating parity band in ^{224}Th was reported to have stable octupole deformation [54]. In Figs. 7(a) and 7(b), it can be seen that the $B(E1)/B(E2)$ values and the δE in ^{74}As are comparable with those in ^{78}Br, but deviate substantially from those in ^{224}Th. These features suggest that octupole correlations exist in ^{74}As. In the $A \approx 80$ mass region, the positive- and negative-parity bands connected by $E1$ in ^{73}Br also indicated octupole correlations [55]. It is suggested that the octupole correlations in ^{73}Br and ^{78}Br were generated from the valence protons occupying the $\pi g_{9/2}$ and $\pi p_{3/2}$ orbits [11,55]. Strong octupole correlations were expected to occur when particle numbers are near 34 ($g_{9/2} \leftrightarrow p_{3/2}$ coupling), 56 ($h_{11/2} \leftrightarrow d_{5/2}$ coupling), 88 ($i_{13/2} \leftrightarrow f_{7/2}$ coupling), and 134 ($j_{15/2} \leftrightarrow g_{9/2}$ coupling) [56]. The proton number for ^{74}As ($Z = 33$) is closer to the particle number 34 than its neutron number ($N = 41$). The occurrence of octupole correlations in ^{74}As are more likely to result from valence protons occupying the $\pi g_{9/2}$ and $\pi p_{3/2}$ orbits. Therefore, band 3 is tentatively assigned the $\pi f_{5/2}/p_{3/2} \otimes \nu g_{9/2}$ configuration.

In summary, high-spin states of ^{74}As were investigated via the reaction ^{74}Ge(^{4}He, $1p3n$). Three $\Delta I = 1$ bands have been identified. Bands 1 and 2 are interpreted as chiral doublet bands. Calculations based on TPRM have been performed to investigate bands 1 and 2, which support the chiral interpretation of the doublet bands. Three $E1$ transitions are observed between bands 1 and 3, combined with the analyses for the $B(E1)/B(E2)$ values and the energy displacement δE, indicating the existence of octupole correlations in ^{74}As. The
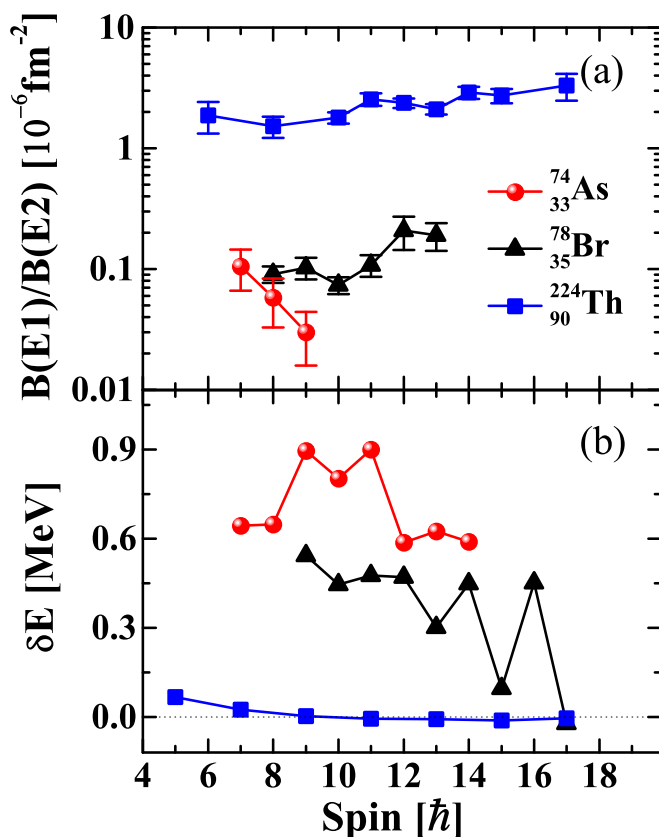

FIG. 7. The experimental $B(E1)/B(E2)$ values (a) and energy displacement δE (b) between bands 1 and 3 as functions of spin in ^{74}As, together with those in ^{78}Br [11] and ^{224}Th [54].

present work extends the border of the chiral nuclei in the $A \approx 80$ mass region to $Z = 33$ and provides a new example of coexistence of chirality and octupole correlations in one nucleus.

[1] S. Frauendorf and J. Meng, Nucl. Phys. A **617**, 131 (1997).

[2] J. Meng, J. Peng, S. Q. Zhang, and S.-G. Zhou, Phys. Rev. C **73**, 037303 (2006).

[3] J. Meng and S. Q. Zhang, J. Phys. G: Nucl. Part. Phys. **37**, 064025 (2010).

[4] R. A. Bark, E. O. Lieder, R. M. Lieder, E. A. Lawrie, J. J. Lawrie, S. P. Bvumbi, N. Y. Kheswa, S. S. Ntshangase, T. E. Madiba, P. L. Masiteng, S. M. Mullins, S. Murray, P. Papka, O. Shirinda, Q. B. Chen, S. Q. Zhang, Z. H. Zhang, P. W. Zhao, C. Xu, J. Meng *et al.*, Int. J. Mod. Phys. E **23**, 1461001 (2014).

[5] J. Meng and P. W. Zhao, Phys. Scr. **91**, 053008 (2016).

[6] A. A. Raduta, Prog. Part. Nucl. Phys. **90**, 241 (2016).

[7] S. Frauendorf, Phys. Scr. **93**, 043003 (2018).

[8] S. Y. Wang, Chin. Phys. C **44**, 112001 (2020).

[9] B. W. Xiong and Y. Y. Wang, At. Data Nucl. Data Tables **125**, 193 (2019).

[10] S. Y. Wang, B. Qi, L. Liu, S. Q. Zhang, H. Hua, X. Q. Li, Y. Y. Chen, L. H. Zhu, J. Meng, S. M. Wyngaardt, P. Papka, T. T. Ibrahim, R. A. Bark, P. Datta, E. A. Lawrie, J. J. Lawrie, S. N. T. Majola, P. L. Masiteng, S. M. Mullins, J. Gál *et al.*, Phys. Lett. B **703**, 40 (2011).

[11] C. Liu, S. Y. Wang, R. A. Bark, S. Q. Zhang, J. Meng, B. Qi, P. Jones, S. M. Wyngaardt, J. Zhao, C. Xu, S.-G. Zhou, S. Wang, D. P. Sun, L. Liu, Z. Q. Li, N. B. Zhang, H. Jia, X. Q. Li, H. Hua, Q. B. Chen *et al.*, Phys. Rev. Lett. **116**, 112501 (2016).

[12] C. Liu, S. Y. Wang, B. Qi, S. Wang, D. P. Sun, Z. Q. Li, R. A. Bark, P. Jones, J. J. Lawrie, L. Masebi, M. Wiedeking, J. Meng, S. Q. Zhang, H. Hua, X. Q. Li, C. G. Li, R. Han, S. M. Wyngaardt, B. H. Sun, L. H. Zhu *et al.*, Phys. Rev. C **100**, 054309 (2019).

[13] X. C. Han, S. Y. Wang, B. Qi, C. Liu, S. Wang, D. P. Sun, Z. Q. Li, H. Jia, R. J. Guo, X. Xiao, L. Mu, X. Lu, Q. Wang, W. Z. Xu, H. W. Li, X. G. Wu, Y. Zheng, C. B. Li, T. X. Li, Z. Y. Huang *et al.*, Phys. Rev. C **104**, 014327 (2021).

[14] L. Mu, S. Y. Wang, C. Liu, B. Qi, R. A. Bark, J. Meng, S. Q. Zhang, P. Jones, S. M. Wyngaardt, H. Jia, Q. B. Chen, Z. Q. Li, S. Wang, D. P. Sun, R. J. Guo, X. C. Han, W. Z. Xu, X. Xiao, P. Y. Zhu, H. W. Li, H. Hua, X. Q. Li, C. G. Li, R. Han, B. H. Sun, L. H. Zhu, T. D. Bucher, B. V. Kheswa, N. Khumalo, E. A. Lawrie, J. J. Lawrie, K. L. Malatji, L. Masebi, J. Ndayishimye, J. F. Sharpey-Schafer, O. Shirinda, M. Wiedeking, T. Dinoko, and S. S. Ntshangase, Phys. Lett. B **827**, 137006 (2022).

[15] Y. Y. Wang, S. Q. Zhang, P. W. Zhao, and J. Meng, Phys. Lett. B **792**, 454 (2019).

[16] Y. Y. Wang, X. H. Wu, S. Q. Zhang, P. W. Zhao, and J. Meng, Sci. Bull. **65**, 2001 (2020).

[17] K. Selvakumar, A. K. Singh, Chandan Ghosh, Purnima Singh, A. Goswami, R. Raut, A. Mukherjee, U. Datta, P. Datta, S. Roy, G. Gangopadhyay, S. Bhowal, S. Muralithar, R. Kumar, R. P. Singh, and M. K. Raju, Phys. Rev. C **92**, 064307 (2015).

[18] S. Guo, C. M. Petrache, D. Mengoni, Y. H. Qiang, Y. P. Wang, Y. Y. Wang, J. Meng, Y. K. Wang, S. Q. Zhang, P. W. Zhao, A. Astier, J. G. Wang, H. L. Fan, E. Dupont, B. F. Lv, D. Bazzacco, A. Boso, A. Goasduff, F. Recchia, D. Testov, F. Galtarossa *et al.*, Phys. Lett. B **807**, 135572 (2020).

[19] R. A. Bark, M. Lipoglavsek, S. M. Maliage, S. S. Ntshangase, and A. Shevchenko, J. Phys. G **31**, S1747 (2005).

[20] M. Piiparinen, A. Ataç, J. Blomqvist, G. B. Hagemann, B. Herskind, R. Julin, S. Juutinen, A. Lampinen, J. Nyberg, G. Sletten, P. Tikkanen, S. Törmänen, A. Virtanen, and R. Wyss, Nucl. Phys. A **605**, 191 (1996).

[21] P. M. Jones, L. Wei, F. A. Beck, P. A. Butler, T. Byrski, G. Duchene, G. de France, F. Hannachi, G. D. Jones, and B. Kharraja, Nucl. Instrum. Methods Phys. Res., Sect. A **362**, 556 (1995).

[22] T. E. Madiba, Directional correlation from oriented states and linear polarization measurements of gamma rays from ^{190}Tl, M.Sc. thesis, University of the Western Cape, 2008 (unpublished).

[23] Y. Oktem, D. L. Balabanski, B. Akkus, C. W. Beausang, M. Bostan, R. B. Cakirli, R. F. Casten, M. Danchev, M. Djongolov, M. N. Erduran, S. Erturk, K. A. Gladniski, G. Gürdal, J. Tm. Goon, D. J. Hartley, A. A. Hecht, R. Krücken, N. Nikolov, J. R. Novak, G. Rainovski, L. L. Riedinger *et al.*, Phys. Rev. C **76**, 044315 (2007).

[24] C. Y. Niu, A. C. Dai, C. Xu, H. Hua, S. Q. Zhang, S. Y. Wang, R. A. Bark, J. Meng, C. G. Wang, X. G. Wu, X. Q. Li, Z. H. Li, S. M. Wyngaardt, H. L. Zang, Z. Q. Chen, H. Y. Wu, F. R. Xu, Y. L. Ye, D. X. Jiang, R. Han *et al.*, Phys. Rev. C **97**, 034322 (2018).

[25] D. A. McCown, L. L. Woodward, and M. L. Pool, Phys. Rev. **74**, 1315 (1948).

[26] E. Eichler, G. D. O'kelley, R. L. Robinson, J. A. Marinsky, and Noah R. Johnson, Nucl. Phys. **35**, 625 (1962).

[27] M. Kaplan, P. Kittel, P. D. Johnston, and N. J. Stone, Nucl. Phys. A **193**, 410 (1972).

[28] J. Christiansen, H.-E. Mahnke, E. Recknagel, D. Riegel, and W. Witthuhn, Nucl. Phys. A **164**, 367 (1971).

[29] B. Lal, Y. K. Agarwal, C. V. K. Baba, S. M. Bharathi, and S. K. Bhattacherjee, Pramana **6**, 209 (1976).

[30] G. García Bermúez, M. Behar, A. Filevich, and M. A. J. Mariscotti, Phys. Rev. C **14**, 1776 (1976).

[31] A. Algora, D. Sohler, T. Fényes, Z. Gácsi, S. Brant, and V. Paar, Nucl. Phys. A **588**, 399 (1995).

[32] S. P. Hu, H. L. Ma, X. P. Cao, X. G. Wu, H. Q. Zhang, H. Hua, J. J. Sun, H. B. Sun, C. Y. He, Y. Zheng, G. S. Li, C. B. Li, S. H. Yao, B. B. Yu, J. L. Wang, H. W. Li, Y. H. Wu, J. J. Liu, P. W. Luo, C. Xu *et al.*, Phys. Lett. B **732**, 59 (2014).

[33] R. A. Haring-Kaye, R. M. Elder, J. Döring, S. L. Tabor, A. Volya, P. R. P. Allegro, P. C. Bender, N. H. Medina, S. I. Morrow, J. R. B. Oliviera, and V. Tripathi, Phys. Rev. C **92**, 044325 (2015).

[34] J. Döring, D. Pantelică, A. Petrovici, B. R. S. Babu, J. H. Hamilton, J. Kormicki, Q. H. Lu, A. V. Ramayya, O. J. Tekyi-Mensah, and S. L. Tabor, Phys. Rev. C **57**, 97 (1998).

[35] K. Starosta, T. Koike, C. J. Chiara, D. B. Fossan, D. R. LaFosse, A. A. Hecht, C. W. Beausang, M. A. Caprio, J. R. Cooper, R. Krücken, J. R. Novak, N. V. Zamfir, K. E. Zyromski, D. J. Hartley, D. L. Balabanski, Jing-ye Zhang, S. Frauendorf, and V. I. Dimitrov, Phys. Rev. Lett. **86**, 971 (2001).

[36] T. Koike, K. Starosta, C. J. Chiara, D. B. Fossan, and D. R. LaFosse, Phys. Rev. C **63**, 061304(R) (2001).

[37] G. Rainovski, E. S. Paul, H. J. Chantler, P. J. Nolan, D. G. Jenkins, R. Wadsworth, P. Raddon, A. Simons, D. B. Fossan, T. Koike, K. Starosta, C. Vaman, E. Farnea, A. Gadea, Th. Kröll, R. Isocrate, G. de Angelis, D. Curien, and V. I. Dimitrov, Phys. Rev. C **68**, 024318 (2003).

[38] T. Koike, K. Starosta, C. Vaman, T. Ahn, D. B. Fossan, R. M. Clark, M. Cromaz, I. Y. Lee, and A. O. Macchiavelli, in *Frontiers of Nuclear Structure*, edited by P. Fallon and R. Clark, AIP Conf. Proc. No. 656 (AIP, Melville, NY, 2003), p. 160.

[39] T. Koike, K. Starosta, and I. Hamamoto, Phys. Rev. Lett. **93**, 172502 (2004).

[40] S. Y. Wang, S. Q. Zhang, Q. Bin, and J. Meng, Chin. Phys. Lett. **24**, 536 (2007).

[41] S. Y. Wang, S. Q. Zhang, B. Qi, and J. Meng, Phys. Rev. C **75**, 024309 (2007).

[42] S. Q. Zhang, B. Qi, S. Y. Wang, and J. Meng, Phys. Rev. C **75**, 044307 (2007).

[43] S. Y. Wang, S. Q. Zhang, B. Qi, J. Peng, J. M. Yao, and J. Meng, Phys. Rev. C **77**, 034314 (2008).

[44] S. Y. Wang, B. Qi, and D. P. Sun, Phys. Rev. C **82**, 027303 (2010).

[45] L. Liu, S. Y. Wang, B. Qi, and C. Liu, Int. J. Mod. Phys. E **22**, 1350060 (2013).

[46] J. Peng, J. Meng, and S. Q. Zhang, Phys. Rev. C **68**, 044324 (2003).

[47] B. Qi, S. Q. Zhang, S. Y. Wang, J. M. Yao, and J. Meng, Phys. Rev. C **79**, 041302(R) (2009).

[48] Q. B. Chen, S. Q. Zhang, P. W. Zhao, R. V. Jolos, and J. Meng, Phys. Rev. C **87**, 024314 (2013).

[49] C. Liu, S. Y. Wang, B. Qi, and H. Jia, Chin. Phys. Lett. **37**, 112101 (2020).

[50] S. Frauendorf, Rev. Mod. Phys. **73**, 463 (2001).

[51] I. Hamamoto, Phys. Rev. C **88**, 024327 (2013).

[52] W. Nazarewicz and P. Olanders, Nucl. Phys. A **441**, 420 (1985).

[53] P. D. Cottle, Phys. Rev. C **41**, 517 (1990).

[54] B. Ackermann, H. Baltzer, C. Ensel, K. Freitag, V. Grafen, C. Günther, P. Herzog, J. Manns, M. Marten-Tölle, U. Müller, J. Prinz, I. Romanski, and R. Tölle, Nucl. Phys. A **559**, 61 (1993).

[55] S. Bhattacharya, T. Trivedi, D. Negi, R. P. Singh, S. Muralithar, R. Palit, I. Ragnarsson, S. Nag, S. Rajbanshi, M. K. Raju, V. V. Parkar, G. Mohanto, S. Kumar, D. Choudhury, R. Kumar, R. K. Bhowmik, S. C. Pancholi, and A. K. Jain, Phys. Rev. C **100**, 014315 (2019).

[56] P. A. Butler and W. Nazarewicz, Rev. Mod. Phys. **68**, 349 (1996).